Exploiting spatial information to estimate metabolite levels in 2D MRSI of heterogeneous brain lesions

Short title: Exploiting spatial information to estimate metabolite levels in MRSI

Anca R. Croitor Sava[a], Diana M. Sima[a], Jean-Baptiste Poullet[a], Alan J. Wright[b], Arend Heerschap[b] and Sabine Van Huffel[a]

[a] Department of Electrical Engineering, ESAT-SCD, Katholieke Universiteit Leuven, Leuven, Belgium

[b] Department of Neurosurgery, University Medical Center, University of Nijmegen, Nijmegen, The Netherlands

Corresponding author: Croitor Sava Anca

ESAT-SCD, K.U.Leuven, Kasteelpark Arenberg 10, postbus 2440, B-3001 Leuven, Belgium,

phone: +32 (0)16 32 11 43, fax: +32 (0)16 32 19 70

E-mail address: anca.croitor@esat.kuleuven.be

Abstract

Magnetic Resonance Spectroscopic Imaging (MRSI) provides MR spectra from multiple adjacent voxels within a body volume represented as a 2 or 3 dimensional matrix, allowing measurement of the distribution of metabolites over this volume. The spectra of these voxels are usually analyzed one by one, without exploiting their spatial context. In this paper we present an advanced metabolite quantification method for MRSI data, in which the available spatial information is considered. A nonlinear least squares algorithm is proposed, where prior knowledge is included in the form of proximity constraints on the spectral parameters within a grid and optimized starting values. A penalty term that promotes a spatially smooth spectral parameter map is added to the fitting algorithm. This method is adaptive, in the sense that several sweeps through the grid are performed and each solution may tune some hyperparameters at run-time. Simulation studies of MRSI data showed significantly improved metabolite estimates after the inclusion of spatial information. Improved metabolite maps were also demonstrated by applying the method to *in vivo* MRSI data. Overlapping peaks or peaks of compounds present at low concentration can be better quantified with the proposed method than with single-voxel approaches. The new approach compares favorably against the multivoxel approach embedded in the well-known quantification software LCModel.

Keywords: quantification, MRSI, spatial information, metabolites

Abbreviations: AQSES, accurate quantitation of short echo time domain signals; HLSVD-PRO, Hankel–Lanczos singular value decomposition with partial reorthogonalization; RMSE, relative mean-squared error; Lip1, lipids at 1.3 ppm; Lip2, lipids at 0.9 ppm; dB, decibel; GMRF, Gaussian Markov random field.

Introduction

Brain tumors in humans occur in a large number of different types, with variable survival prospects and requirements for treatment. The most common type, gliomas, has a very unfavorable prognosis. Magnetic Resonance Imaging (MRI) is widely used in the clinic for differential diagnosis and prognosis of brain tumors, but with conventional MRI, essentially assessing anatomy, this is often difficult. Therefore, more functional MR approaches, such as MR spectroscopy (MRS), are explored to investigate specific characteristics of brain lesions. MRS has been shown to offer significant metabolic information that is useful for clinical diagnosis and treatment evaluation and in pre-clinical investigations of tumors. Magnetic Resonance Spectrocopic Imaging (MRSI) is an MR technique that combines MRS and MR imaging methods by measuring MR spectra of a 2 or 3 dimensional array of voxels. It facilitates the observation of the spatial distribution of metabolic patterns over tumor and surrounding tissue regions, which is important because of the heterogeneous nature of tumors. The results of MRSI measurements can be exploited in tissue segmentation and classification techniques, which may be used for the quantification of tissue volumes, and localization and spatial characterization of the heterogeneous lesions in tumor tissue (1-5). This can play an important role in pre-surgical and (radio-)therapy planning. In practice the result of tissue segmentation should be part of a clinical decision support system able to improve the quality of clinical decision making, offer better diagnosis, prognosis and treatment selection of brain tumors.

When classifying brain tumors using MRSI data, the input used by the pattern recognition techniques are either the full spectra or a set of metabolic features extracted from the spectra. Still, due to computational matters, using the metabolite tissue concentrations as input features is preferred, as previous studies reported high accuracy with such feature-based classification approaches (4, 6, 7). Since metabolite concentration estimates from MRSI

signals are the input variables for advanced classifiers for tissue type differentiation and tumor recognition, it is clear that reliable quantification results are very important. The problem of quantifying metabolite concentrations from *in vivo* single voxel MRS measurements has been tackled by a variety of model-based methods, both in time and frequency domain, such as VARPRO (8), AMARES (9), LCModel (10, 11), TDFDfit (12), QUEST (13) and AQSES (14). These methods are initially designed to work on individual voxels and when applied to MRSI data the signals from each voxel within the MRSI grid are quantified separately. As opposed to single-voxel measurements, the MRSI signals usually have a lower quality, due to the spatial/spectral trade-off for the available measuring time. Thus, although MRSI is getting more and more popular in the MR community, retrieving accurate estimates of the most relevant metabolite concentrations remains a challenging computational task because of magnetic field inhomogenieties, relatively low signal-to-noise ratio (SNR) and physiological motion, compromising spectral resolution, and strongly overlapping metabolite peaks. Since MRSI provides measures of multiple metabolites simultaneously at each voxel, there is furthermore great interest in exploiting the available spatial information, as this is expected to improve the accuracy of quantification compared to processing the signals on an individual voxel basis.

Incorporating spatial prior knowledge to optimize processing of MRSI data has been addressed previously (15-17). The prior knowledge that has been considered so far includes the assumption that the signals are perfectly aligned in frequency and/or the phase of the resonances is constant over the grid under proper preprocessing (15), that the frequency, damping and phase parameters have spatially smooth variations (16), that the metabolite composition of each tissue type is relatively constant over a local region and MRI-derived tissue distribution functions can be used as prior knowledge for MRSI quantification (17). In all these approaches a common quantification solution is formulated for the whole MRSI grid assuming that many characteristics of the signals within the same grid are related. Still

differences in the signals may appear due to the heterogeneity of the tissue under investigation and inhomogeneities in the magnetic field applied in the scanner. It is well-known that some metabolite concentrations differ with tissue type. For example the compound N-Acetyl Aspartate (NAA) is reduced in voxels containing tumor tissue as compared to normal tissue (18, 19). Moreover, T2 relaxation times of metabolite spin systems may also depend on tissue type (20, 21) and pathology (22). At the same time, the spectral parameters such as damping and frequency are magnetic field-dependent. The process called shimming aims to obtain a constant magnetic field throughout the MRSI grid. Although an optimal shimming result is not guaranteed, it is reasonable to assume that there are no abrupt changes in the magnetic field between neighboring voxels and that possible variation in the damping and frequency parameters proceed smoothly over the considered MRSI grid. Exceptions could be the occurrence of abnormal features strongly affecting susceptibility, such as bleeds or cysts or for voxels at sharp boundaries like the borders of ventricles.

In this paper we propose a novel approach: an alternating nonlinear least squares algorithm for fitting and modeling MRSI data, in which both the parameters' variability and similarity within an MRSI grid are considered. In the quantification of all voxels, penalties are added to promote, within neighboring regions, smooth parameters maps for frequency shifts and damping corrections, while allowing complete freedom to the metabolite amplitudes (tissue concentrations). Due to the heterogeneity of the tissue that characterizes brain tumors, and to the variations induced by magnetic field inhomogeneities, a common optimization over the whole MRSI array is not explicitly formulated, as opposed to previous studies (15-17). We use a dynamic approach, in which the bounds on the relevant values of the parameters are iteratively adapted, and/or the parameters of the model function take new starting values for each voxel, at each iteration. To assess the quality of our method, an extensive Monte Carlo simulation study and several *in vivo* MRSI examples of brain tumor patients are presented.

1. Methods

The method we propose is an important extension of the time-domain quantification method AQSES (Accurate Quantitation of Short-echo Time Magnetic Resonance Spectroscopic Signals) (14) for MRSI data, aiming to exploit spatial knowledge present in the data. AQSES fits the measured signal to a nonlinear model (23), which is derived from metabolite profiles that are measured *in vitro* or quantum-mechanically simulated. The AQSES optimization problem is further modified in order to account for the spatial prior knowledge available when dealing with MRSI data. We further refer to the new version as AQSES-MRSI. The method is embedded as a plugin to the in-house software SPID (24), a Matlab® (The MathsWorks™) platform for advanced spectroscopic signal preprocessing, processing and classification.

1.1 Single voxel quantification based on a metabolite basis set

MRS and MRSI signals are measured in the time-domain and are Fourier transformed for better visualization into frequency-domain spectra. In most quantification methods an appropriate nonlinear model is fitted to the measured MRS signal by minimizing the sum of the squared residuals, which is the maximum likelihood solution under the assumption of additive white Gaussian noise. The fitting can be done in the time domain (9, 13-14), in the frequency domain (10, 11), or by combining both domains (12).

In AQSES (14) the free induction decay (FID) signal is modeled as a linear combination of K possibly damped, phase and frequency-shifted metabolite templates. We consider that we are given a "metabolite basis set" as a set $\{\nu_k$, for $k = 1,...,K\}$ of complex-valued signals of length N, representing *in vitro* measured or quantum mechanically simulated NMR responses

of pure metabolites. An *in vivo* NMR signal *y*, which is also a complex-valued time series of length *N*, is assumed to satisfy the model:

$$y(t) = \hat{y}(t) + \varepsilon_t \text{ , } t = t_0, \ldots t_{N-1} \quad [1]$$

$$\hat{y}(t) = \sum_{k=1}^{K} \alpha_k \varsigma_k^t \eta_k^{t^2} \nu_k(t) + b(t) + w(t) \quad [2]$$

where α_k, ς_k, $\eta_k \in$ C are unknown parameters that account for amplitudes of the metabolites in the basis set and for the necessary corrections of the basis set signals. The complex amplitudes α_k and the complex values ς_k and η_k can be written as (with $j = \sqrt{-1}$) (23):

$$\alpha_k = a_k \exp(j\phi_k)$$

$$\varsigma_k = \begin{cases} \exp(-d_k + 2\pi j f_k) & \textit{for Lorentzian and Voigt lineshapes} \\ \exp(2\pi j f_k) & \textit{for Gaussian lineshapes} \end{cases}$$

$$\eta_k = \exp(-g_k) \qquad \textit{for Gaussian and Voigt lineshapes}$$

where a_k are positive real-valued amplitudes, ϕ_k are the phase shifts, f_k are frequency shifts, d_k are Lorentzian damping corrections, and g_k are Gaussian damping corrections. In [1], the term ε_t denotes an unknown noise perturbation with zero mean. In [2], *b(t)* denotes the "baseline", which is the response of macromolecules that are not included in the basis set, and *w(t)* denotes the water component. For ease of exposition, the analysis in this paper is restricted to the assumption that the water and baseline contributions have been filtered out in a preprocessing step.

Typically, the single voxel time-domain quantification problem can be expressed as:

$$\min_{\varsigma_1,\ldots,\varsigma_K,\eta_1\ldots,\eta_K} \frac{1}{N} \sum_{t=t_0}^{t_{N-1}} \left| y(t) - \sum_{k=1}^{K} a_k \exp(j\phi_0) \varsigma_k^t \eta_k^{t^2} \nu_k(t) \right|^2 \quad [3]$$

This nonlinear least squares problem can be solved separately for each signal of MRSI data, without taking into account any spatial information. From a computational point of view, we only focus on the damping corrections and frequency shifts of all metabolites, which can be stacked in a vector θ. This comes from the fact that AQSES is implemented as a separable problem using a variant of the variable projection method (23), which means that the parameters appearing linearly into the model (the complex amplitudes α_k, yielding the real-valued amplitudes and phases) are projected out, since they are uniquely determined through a linear least squares problem by the values of the nonlinear parameters.

1.2 Modalities of exploiting spatial information

If we consider a voxel *c* within an MRSI grid of voxels, smooth parameter maps can be locally measured at voxel *c* by using the parameter value at the current location and the values in a certain neighborhood. AQSES-MRSI starts by individually fitting each signal in the grid using nonlinear least squares (14, 23). Then several sweeps through the grid are performed until convergence. At each sweep spatial information is taken into account in the fitting algorithm by imposing smoothness constraints in more steps, outlined below and explained in Section 1.3 in full details:

-1st step: in this step changes are made to the starting values of the nonlinear parameters, θ_c (vector containing damping corrections and frequency shifts for voxel *c*), to be set to the median of the parameter values from the considered neighbors θ_s, obtained in the previous sweep ($s = 1,\ldots,S$, where S is the total number of voxels in the considered neighborhood).

-2nd step: this step optimizes the bounds on the parameters' variability. We add an extra box constraint so that the parameters of the neighboring voxels do not present a high variability. The upper and lower bounds of this constraint are imposed by

tightening the previous box based on the current information available in the neighboring voxels.

-3rd step: in this step spatially smooth parameter maps for the frequency shifts and damping corrections are imposed. The nonlinear least squares problem is modified by adding a penalty term, which builds a sum over the squared distances between the parameters of all neighboring voxels. The weight on the smoothness of individual parameters is adjustable.

The convergence

The convergence measure is defined at each sweep *i* as:

$$C_i = \frac{1}{PL}\sum_{l=1}^{L}\sum_{p=1}^{P}\frac{\left(\theta_l^{\,i}(p)-\theta_l^{\,i-1}(p)\right)^2}{\theta_l^{\,i}(p)^2},$$

where $\theta_l^{\,i}(p)$ is the estimated parameter p of signal l in sweep i, P is the number of parameters per signal, L is the number of signals. The iterative algorithm continues until $C_i<0.001$ or we reached the maximum of 10 sweeps. Still we observed that the convergence is typically reached in less than 10 sweeps.

1.3 The quantification method AQSES-MRSI

In the single voxel implementation of AQSES, it was found convenient to set to zero all the initial values of the nonlinear parameters (frequency and damping corrections). In this way the optimization starts with no spectral correction with respect to the signals from the metabolite basis set. The latter are assumed to be reasonably aligned to the *in vivo* signals. In AQSES-MRSI we introduce spatial information by initializing the nonlinear parameters of the voxel of interest with the median value of parameters in the previous sweep from the

voxels considered in the selected neighborhood area. The first sweep uses initial values equal to zero.

$\theta_c^i = median(\theta_s^{i-1})$, where

θ_c^i represents the starting values of the nonlinear parameters at sweep *i*,

θ_s^{i-1} represents the optimal parameters of the surrounding voxel *s* obtained at sweep *i-1*.

In the 2nd step we introduce an effective spatial constraint such that the parameters of the neighboring voxels do not yield a high variability. AQSES itself uses soft constraints (i.e., reasonable bounds on the damping and frequency corrections) of the form $d_k \in [0, A_d]$, $f_k \in [-A_f, A_f]$, where A_d and A_f are small scalar values. Recall that the nonlinear parameters represent corrections applied to the metabolite profiles. These soft constraints can be written in vector form as a box constraint: $\theta_c \in [B_{low}, B_{up}]$. The allowed parameter variation in this step of AQSES-MRSI is bounded by the following interval:

$$\theta_c^i \in [\overline{\theta}_s^{i-1} - \alpha^{i-1} B_{low}, \overline{\theta}_s^{i-1} + \alpha^{i-1} B_{up}]$$

where α^0 is a scalar value initially set to 0.25, $\overline{\theta}_s^{i-1}$ is computed at sweep *i* as the mean of the damping and, respectively, frequency of the voxels surrounding the voxel of interest and estimated in the sweep *i-1*. The value of α^i decreases with each sweep as $\alpha^i = \alpha^0 / i$, where *i* is the sweep counter.

Finally, in the 3rd step, inspired by (16), a penalty term over the parameter maps is formulated. With AQSES-MRSI a complex optimization problem is considered by imposing a trade-off between solving the minimization problem as described in [3] and minimizing the nonlinear parameters variation within neighboring regions:

$$\min_{\theta_c} \frac{1}{N} \sum_{t=t_0}^{t_{N-1}} \left| y_c(t) - \hat{y}_c(t,\theta_c) \right|^2 + \sigma^2 \sum_{\theta_c \neq \theta_s} \varepsilon_s \beta_{cs} \left\| W(\theta_c - \theta_s) \right\|_2^2 \qquad [4]$$

where the signal $y_c(t)$ corresponds to voxel *c* and the model $\hat{y}_c(t,\theta_c)$ is considered as a weighted sum of metabolite signals with nonlinear corrections θ_c. Spatial information is introduced via the second term, called penalty term, which encourages a smooth solution for the problem (16). The penalty terms are multiplied by adjustable scalar penalty parameters ε_s, which account for the trade-off between an optimal fitting of the current signal and the penalty.

σ^2 is an estimate of the noise variance computed from the tail of the signal in time domain in voxel *c*. β_{cs} is a weighting scalar which gives the influence of the parameters θ_s on the parameters θ_c, as described below. *W* is a diagonal weighting matrix, with $W \in R^{Km \times Km}$, which accounts for the scale differences between parameters, where *K* is the number of metabolite profiles and *m* is the number of parameters per metabolite. For example, for the Lorentzian model, m=2 (damping and frequency), if we use variable projection and solve for amplitude and phase in closed form. Thus *W* can be used to adjust the weight on the smoothness of certain individual parameter maps and even to turn off smoothing for some of the parameters by using a zero weight. In summary, all the parameters in the penalty term, ε_s, σ^2, *W* and β_{cs}, determine the trade-off between fitting the individual signals against smoothing the parameter maps.

The spatial model

Following the work of (25), we apply a sliding window method, i.e., the sweeps go through the voxels row-wise (a checker-board pattern or a spiral starting from the center of the grid are also possible). In choosing the geometry of the neighborhood, different models can be

used for introducing spatial information in the optimization problem (26). Yet, based on the assumption that tissue and magnetic field inhomogeneities influence the parameter maps, spatial constraints are further considered only within the voxels surrounding the voxel of interest, restricting in this way the neighborhoods to small areas. Throughout the 2D experiments the "3x3 spatial model" (the adjacent voxels plus voxels on the diagonal are considered as neighbors, giving a total of 8 voxels (26), see Figure 1-a) is used. An extension to the 3D MRSI case could be possible. The selection of a fixed neighborhood (26) can be a disadvantage, in particular for very heterogeneous data. To overcome this limitation, we introduced an extra decision factor in the proposed method, β_{cs}, which makes the process of selecting the neighborhood more flexible. AQSES-MRSI allows the user to account for both the similarities and the variability within an MRSI grid.

Defining the weighting scalar β_{cs}

The spatial information is taken into account via:

$$\beta_{cs} = \beta_{cs}^{neighborhood} \beta_{cs}^{tissue}$$

where $\beta_{cs}^{neighborhood}$ is 0 or 1 depending on whether voxels *c* and *s* are neighbors according to, e.g., the "3x3 spatial model" for selecting the neighborhood area, see Figure 1-a.

β_{cs}^{tissue} is based on tissue information and reflects how similar two voxels *c* and *s* are, independently from spatial consideration. The higher β_{cs}^{tissue}, the higher the influence of voxel *s* on voxel *c*, in other words, the closer the parameters θ_c and θ_s should be. To simplify, one can use $\beta_{cs}^{tissue} = 1$ if tissue type is similar, and $\beta_{cs}^{tissue} = 0$ otherwise. β_{cs}^{tissue} has to be available as prior information (Figure 1-b). It can be obtained previously via MRI segmentation or classification. This segmentation procedure is not part of this study.

Choosing the weighting matrix *W*

The diagonal matrix *W*, which accounts for the different scales and variability of the parameters, can be used to adjust the smoothness of individual parameter maps. Let

$$W = \begin{pmatrix} W_d & 0 & \dots & 0 & 0 \\ 0 & W_d & \dots & 0 & 0 \\ \dots & \dots & \dots & \dots & \dots \\ 0 & 0 & \dots & W_f & 0 \\ 0 & 0 & \dots & 0 & W_f \end{pmatrix}$$

where $W \in R^{Km \times Km}$. We consider equal weights for all damping corrections and equal weights for all frequency shifts. Both for simulation experiments as well as for *in vivo* data $W_d = 0.2$ is used for the Lorentzian damping parameters and $W_f = 2$ for the frequency maps (16).

Choosing the penalty parameters ε_s

The positive scalar parameters ε_s accounts for the trade-off between fitting the model $\hat{y}_c$ to the signal y_c in least squares sense and imposing the minimization of the penalty term. We allow ε_s to be adaptively chosen for each particular signal at each sweep by evaluating the current residual sum of squares $RSS = \frac{1}{N}\sum_{t=t_0}^{t_{N-1}} \left| y_c(t) - \hat{y}_c(t,\theta_c) \right|^2$ and the current penalty norm $penalty_s = \left\| W(\theta_c - \theta_s) \right\|_2^2$ and setting $\varepsilon_s = 0.1\sqrt{RSS} / \sqrt{penalty_s}$, which gives 90% importance to the fit and 10% importance to the penalty.

Performance measures

To evaluate the robustness and performance of the method a simulation and an *in vivo* experiment were designed.

Firstly, Monte Carlo studies were performed on a series of 225 MRSI simulated signals grouped in 25 simulated MRSI grids of dimension 3x3 voxels. To analyze the performance of the proposed method for different levels of noise, white Gaussian noise with different levels of SNR was added to the signals. The signal power, $P_{\underline{sig}}$, was measured for each signal as the squared Euclidean norm of the time-domain signal divided by the length of the signal, and transformed to dB through $P_{\underline{sig}} := 10\log_{10}(P_{\underline{sig}})$. Then the standard deviation of the added noise, *N(t),* for the different levels of SNR was computed as:

$$std_{N(t)} = \sqrt{10^{\left(\frac{P_{sig} - SNR}{10}\right)}}$$

Figure 2 illustrates how the different levels of SNR (10, 15, 20, 25 and 30) perturb the signals. For this experiment, damping, frequency and amplitude values were set to take values corresponding to the signals measured in normal brain tissue. These nominal values were chosen as in (14) and are within the intervals reported for *in vivo* MRSI (19, 29). Typically, before quantifying *in vivo* MRSI data, a phase-correction preprocessing step is performed. Assuming phase-corrected *in vivo* MRSI data, within the same grid, the phase values are kept constant for the same metabolite profile. Randomly valued, but reasonably smooth parameter maps were considered for damping and frequency so that, for each metabolite, the distortions of the exponential damping factor are limited to ±15% from its nominal value *d* within the MRSI grid. Thus, the damping values for each metabolite uniformly cover the interval [*d – 0.15*d, d + 0.15*d*]. Similarly, frequency shifts are allowed a variation of ±10%, [*f–0.1*f, f+0.1*f*].

The relative mean-squared error (RMSE) was computed for each metabolite *k* within the simulated grid, as follows:

$$RMSE_k = \left(\frac{1}{L} \sum_{l=1}^{L} \frac{(\hat{a}_{k,l} - a_k^{sig})^2}{\left(a_k^{sig}\right)^2} \right)$$

where $\hat{a}_{k,l}$ is the estimated amplitude of the l^{th} signal and a_k^{sig} is the true amplitude. *L* is the number of signals within the MRSI grid.

The performance over the whole grid and over all metabolites is computed as:

$$RMSE = \left(\frac{1}{K} \sum_{k=1}^{K} RMSE_k \right),$$

where *K* defines the number of metabolites.

For every specific test we compute the corresponding Cramer-Rao lower bounds (CR bound) from the Fisher information matrix corresponding to the true parameter values of the nonlinear model function. Then, we compare the calculated *RMSEs* with the theoretical CR bounds. This gives us an excellent indication of the gain in the accuracy that can be obtained by using AQSES-MRSI.

In order to analyze the effect of sharp edges versus smoothness and the influence of different levels of inhomogeneities on the performance of AQSES-MRSI, a 2nd simulation experiment was designed. For this purpose four MRSI data sets of 10x10 voxels have been generated with different parameter maps. Each simulated MRSI grid containing a region with normal-tissue-like spectra and a region with tumor-like spectra. We considered parameter maps with: A. sharp edges but constant parameter values within a tissue region and different between the regions; B. sharp edges with slightly varying random parameters values within the tissue region, but highly different between the regions; C. sharp edges with smooth parameter map within the tumor region, and D. smooth edges with smooth parameter maps over the whole grid. Gaussian white noise of SNR = 15 was added to all signals. $RMSE_k$ and *RMSE* were computed for each data set.

Thirdly, to verify to which extent the conclusion drawn in the simulation studies are consistent with real conditions, in other words, to analyze whether the method preserves its

robustness and accuracy when applied to real data, *in vivo* studies are performed. To this end we apply the method to several *in vivo* MRSI measurements. The cases are extracted from the INTERPRET database (27). As an illustration we present and discuss the quantification results coming from three patients diagnosed with different tumor types. The performance of AQSES-MRSI on *in vivo* MRSI cases is compared with the single voxel time domain quantification methods AQSES (14) and QUEST (13), the latter being a well-known quantification method included in the jMRUI tool (28), applied on individual voxels. We also compared our results with LCModel (11), which incorporates a functionality that allows the user to consider spatial information when analyzing multivoxel data. When quantifying the *in vivo* MRSI data with LCModel, the same metabolite basis set as for the other methods was considered. As explained in LCModel's User Guide, prior information of phase and frequency adjustments from one voxel are included as soft constraints for the next voxel in a row-by-row analysis. These are preceded by locating Cho and NAA peaks for a "preliminary analysis" for the improved estimation of phase and frequency adjustments. The final full analysis calculates relative concentrations of metabolites across all voxels. To asses the quality of the fit, the quantification results are translated into metabolic maps. Additionally, an analysis of the fit and of the residual is performed.

2. Materials

2.1 Simulation experiments

The simulated signals were obtained as a linear combination of 11 metabolite profiles, which were individually shifted in frequency and broadened as described in the previous section: nine measured metabolite profiles: NAA, myo-inositol (Myo), creatine (Cr), phosphocholine (PCh), glutamate (Glu), lactate (Lac), alanine (Ala), glucose (Glc), taurine (Tau) plus two simulated lipids profiles: lipids at 1.3ppm (Lip1) and lipids at 0.9ppm (Lip2) (13). The measured profiles were selected from a measured database acquired with a 1.5 T Philips NT

Gyroscan using a PRESS sequence with an echo time of 23 ms, and a PRESS box of 2 *x* 2 *x* 2cm^3, as described in (14).

2.2 *In vivo* MRSI studies

The MRSI data were acquired in the Radboud University of Nijmegen Medical Centre (RUNMC) on a 1.5T clinical MR system (Siemens Vision), using a 2D STEAM pulse sequence with the STEAM box positioned in a transversal plane through the brain showing the largest tumor diameter in the Gd contrast enhanced image. The study was approved by the ethical committee of the UMCN and for tumor typing followed the rules of the World Health Organization (WHO). The MRSI parameters are: 16x16x1024 samples, TR/TE/TM=2000 or 2500/20/30 ms, slice thickness = 12.5 or 15 mm, FOV (field of view) = 200 mm, spectral width = 1000 Hz. The water suppressed MRSI signals are preprocessed as follows: filtering of k-space data by a Hanning filter of 50% using the LUISE software package (Siemens, Erlangen, Germany), zero filling to 32 x 32 and spatial 2D Fourier transformation to obtain time domain signals for each voxel, Eddy current correction, water removal with HLSVD-PRO (30) and baseline correction performed as described in (24). Finally, all spectra were normalized with respect to the amplitude of the water unsuppressed signal. The SNR of the preprocessed data is computed as the power of the signal, $P_{sig,}$ after extracting the estimated noise power, divided by the power of noise, $P_{noise,}$ computed from the last 180 points of the time-domain signals. For the considered data, SNR values are between 8 and 16 dB.

As in the simulation study, 9 measured metabolites and 2 simulated ones were considered for quantifying the data. The measured metabolite profiles were selected from a measured basis set acquired on a 1.5 T Siemens system, using a STEAM sequence with an echo time of 20 ms, and a STEAM box of 2x2x2 cm^3, as described in (14). These metabolites were chosen based on their potential as biomarkers to separate between different brain tissue types as well as to identify brain lesions. Another important aspect in the choice of a restricted basis set is that fitting metabolites that are actually not visible in the spectrum or that are too correlated

with each other may increase the complexity of the problem and affect the accuracy of the algorithm (14). AQSES-MRSI can be combined with any other simulated or measured basis set under the same protocol as the considered *in vivo* data and the basis set given here is just a representative example.

3. Results

3.1 Monte Carlo simulations

First we analyze the improvement brought in by introducing spatial information at different levels in the fitting algorithm. The results are presented with respect to different noise levels, see Figure 3, and compared with the single-voxel approach AQSES. This is done separately for the sequential steps of the algorithm (see Section 1.2) so that we can observe how each step aimed at introducing spatial prior knowledge influences the quantification results. For low level of noise both AQSES and AQSES-MRSI 1st, 2nd and 3rd step prove to be very robust and accurate as the RMSE curves almost converge to the CR bound values.

For higher levels of noise, we observe a clear difference between the performance obtained with the individual voxel approach versus the multivoxel approach. From the results we can conclude that incorporating spatial information in the form of dynamic starting values for nonlinear parameters contributes in minor percentage to the final performance reached by AQSES-MRSI, as a small improvement in the accuracy is obtained after this step (see AQSES-MRSI$_{1st\ step}$). The gain in accuracy becomes obvious after the 2nd step where we impose soft constraints on the damping and the frequency parameter maps (see AQSES-MRSI$_{2nd\ step}$). After the 2nd step, the accuracy with respect to the single-voxel approach improves with up to 70% at low SNR. At high noise levels (see Figure 3), the last step, which imposes smoothness penalties, AQSES-MRSI$_{3rd\ step,}$ brings an improvement of 78% in the accuracy.

We also investigated the performance of AQSES-MRSI for each metabolite individually, (Figure 4). A major improvement in estimating the overlapping metabolites (Lip1, Lip2, Lac and Ala) is obtained with the proposed method. Low standard deviation values with respect to the mean performance are registered with AQSES-MRSI proving that the problem of metabolite mis-quantification is reduced. Indeed, these peaks are strongly overlapping with other metabolites, thereby decreasing the robustness of metabolite estimation. In contrast, AQSES-MRSI still provides good estimates showing that by using spatial constraints in the fitting algorithm we are able to obtain robust parameter estimation of overlapping peaks; see Figure 5 for the RMSEs of these metabolites for a range of SNRs.

To estimate the impact of using spatial information in quantifying inhomogeneous data we further present the results obtained with AQSES-MRSI in the second experiment, where four sets of simulated MRSI grids presenting different types of parameter maps were used. The results of this experiment are presented in Figure 6. Regardless of the degree of inhomogeneity, AQSES-MRSI outperforms the single voxel approach. The RMSE for AQSES-MRSI stays constantly below 3 within the MRSI grid. For the voxels situated at the interference between the two considered tissue types we can notice some problems for the sharp edge maps (see map A and map B). Even if the error remains low in these regions, the performance of the algorithm is influenced by sudden parameters change.

The error in estimating the metabolite concentrations for map D are detailed in Figure 6.b-c. A percentage of improvement of up to 75% is reported when using AQSES-MRSI. The estimates obtained with AQSES-MRSI are very close to the true amplitudes regardless of the tissue type. AQSES performance shows to be tissue type dependent (see the error maps of the following metabolites: Cr, Lac, Lip1, Lip2, Ala, in Figure 6c). This drawback is a consequence of the fact that metabolite concentration varies with the tissue type and,

therefore, metabolites in low concentration in a certain region can not be estimated with high accuracy with a single voxel approach. With AQSES-MRSI this problem is reduced.

3.2 Effect of including spatial prior knowledge on analyzing i*n vivo* MRSI data

We showed in the simulation studies that by including prior knowledge in the form of spatial constraints, the accuracy of estimating metabolite concentrations improves. Now we further analyze the performance of AQSES-MRSI on *in vivo* MRSI data.

Metabolic maps

We present the results obtained with AQSES-MRSI on three patients with different tumors (a meningioma, a glioblastoma and an oligoastrocytoma tumor grade III). Similar results were obtained for other patients within the INTERPRET database (31). Since this study is not aimed at evaluating a preliminary MRI segmentation step, when defining the parameters β_{cs}, tissue class prior knowledge is not included. This means that we impose the spatial constraints on all the voxels surrounding the voxel of interest as defined with the 3 x 3 spatial model (see Section 1.3). The resulting metabolite estimates are exported into metabolite maps. By analyzing these maps we can have a fast visual overview on the performance of the method. We emphasize that no post-smoothing has been performed on the metabolite map images.

For all cases, the proposed method provides a much less noisy spatial distribution for the metabolites, with well-contoured metabolic maps, as opposed to AQSES, QUEST and LCModel. Even for metabolites that are difficult to quantify with conventional approaches we obtain good results, as can be seen in Figures 7-9.

For the meningioma patient, AQSES-MRSI results are in agreement with previous studies, (e.g. 19, 32, 33) and in the tumor area the NAA, Cr and Myo levels are lower with respect to

the non-affected area, while Glc levels are higher. The Myo and Glc metabolite maps drawn based on the results obtained with the single-voxel approaches are noisier and a clear differentiation between the normal and tumor tissue is not obtained when analyzing the levels of these compounds over the whole grid (Figure 7). A decrease in NAA and Cr in the tumor area is observed for all four approaches. Still, a smoother map is obtained when using spatial prior knowledge. Compared to LCModel, similar metabolite maps were obtained for NAA, Cr and Myo. The LCModel map for Glc is in disagreement with all the other results and with the literature (32).

For the patient with a glioblastoma (Figure 8), Ala and Lac concentration estimates with AQSES-MRSI are increased in the tumor region while NAA is low, which has been observed in previous studies for these tumors (e.g. 19, 34). Lips levels are reported by all methods as elevated in the affected area, being very high towards the center of the tumor area which could be a sign of necrotic tissue (19, 35). Also in this example, the parameter maps obtained with AQSES, QUEST and LCModel are less smooth. For the single voxel approaches, high levels of Ala and Lac are present in isolated voxels in the normal tissue region, not likely to represent the true situation, but rather artifacts due to mis-fitting. Compared to AQSES-MRSI, LCModel, which considers spatial knowledge, provides smooth metabolites in the normal tissue region, while for the tumor region the maps are very noisy and present variations that seem to be above the limit of a normal inhomogeneity behavior (the metabolite value in a voxel within the tumor tissue region is closer to the mean of the metabolite value within the normal tissue region). A better fit is observed with AQSES-MRSI for the spectra coming from tumor regions, where the residual presents no contribution from the considered metabolites. With AQSES-MRSI the tumor region is nicely contoured and the whole grid gives a smooth overview over the whole investigated image. These results are also closer to the diagnosis agreed by the clinicians after the histopathology. Moreover, the metabolite

maps seem more plausible when using the proposed spatial prior than without it, which is justified by comparing spectra of neighboring voxels.

For the oligoastrocytoma case the quantification results allow us not only to separate between tumor and normal tissue region, but also to find the contour of the CSF zone. When analyzing AQSES-MRSI results from the quality-of-fit point of view we observe high performance both in the tumor and in the normal tissue region. As an illustration, two signals from different tissue regions are presented together with their AQSES-MRSI fit and the residual, see Figure 9. The residuals do not exhibit obvious unassigned metabolite peaks.

4. Discussion

In this study we developed a new, fully automated method, called AQSES-MRSI, to estimate metabolite levels in MRSI data, that includes spatial information of neighboring voxels, and demonstrated its enhanced performance with respect to the time-domain quantification methods AQSES and QUEST, both working on a single-voxel basis. An analysis of MRSI data by LCModel software, which also includes spatial information, showed a relatively low performance in tumor regions, suggesting that its accuracy is tissue type dependent, which could be a drawback in the processing of very heterogeneous MRSI data

An important advantage of using spatial prior knowledge in the quantification of MRSI spectra is that overlapping peaks as Ala, Lac and Lip_s can be better assessed independently, also in cases where single-voxel approaches fail to do so. This can represent a critical point in the quantification of MRSI data and further in the classification of brain tumors based on spectroscopic MR signals, as we know that these peaks are important biomarkers to discriminate different tissue types. In addition, resonances of metabolites present at relatively low concentration can be better estimated. This represents an added value in the analysis of MRSI data for the detection and characterization of brain lesions and disorders, as most of the

classification algorithms are applied on feature vectors derived from tissue levels of relevant metabolites. Application of the new method to brain tumors, which can be very heterogeneous, showed improvements compared to conventional processing methods. Thus it is expected that starting from more reliable spectral parameter estimates the accuracy and robustness to separate tumor and normal tissue and to differentiate between tumor types will be enhanced. AQSES-MRSI results can be used as more robust starting points towards improved tissue segmentation and classification.

The simulation studies showed that by exploiting spatial prior knowledge and by using information from the spectral parameters (frequencies, dampings) of spectra from surrounding voxels, statistically better results are obtained compared to processing the signals on an individual basis. The spectral resolution of the *in vivo* data sets was too low to permit proper differentiation between Glu and Gln; the Cramer-Rao lower bounds were larger than 50% for each of the two metabolites. However, the sum of Glu and Gln could be reasonably estimated.

Previous quantification studies that exploit spatial prior knowledge demonstrated that this information can improve the estimation of metabolite levels (15, 16). The approach proposed in (15) extends the AMARES$_{ts}$ method (Advanced Method for Accurate, Robust and Efficient Spectral fitting - time series approach) (36) and exploits the idea of processing the spectra within the MRSI grid simultaneously, while equating some spectral parameters across the grid. The problem is seen as a quantification of a series of MRS signals, which boils down to minimizing a cost function that includes more signals simultaneously. In (15) it is assumed that the frequencies and phases remain constant over the whole MRSI grid, thus equality relations between these parameters of the same type are imposed for all signals. The signals need to be preprocessed by eddy current correction and spectrum alignment such that these assumptions are sufficiently met. Then the model function is used for all the voxels, but the

number of free model parameters is lowered due to the imposed equalities on frequencies and phases, respectively, across all voxels. However, the distortion of the nonlinear model parameters of *in vivo* MRS signals depends on magnetic field inhomogeneities. These are, in turn, also dependent on the heterogeneity of the tissue. Hence, such a simplified solution does not satisfy the complexity of the problem in realistic cases. To better meet such conditions small variations in the frequency shifts are allowed in AQSES-MRSI, and smooth parameter maps are imposed for the damping corrections.

In another study spatial information is being used by a hierarchy of neighborhood systems in the form of a generalized Gaussian Markov random field (GMRF) (16). Instead of exact equality relations, softer constraints are considered in the form of spatially smooth parameter maps for the frequencies, dampings and phase variables. To this end, a Bayesian approach of specifying a prior distribution over the considered parameter maps is used (37). This means that penalty terms in the form of weighted distances between parameters of the same type are added to the nonlinear least squares fitting problem based on the classical model of a sum of damped exponentials. As in (15) the optimization function is modified so that several signals are fitted simultaneously and the method is not sensitive to the heterogeneity of the information contained in the MRSI grid. Although GMRF provide an elegant methodology, the structure of the GMRF is often a poor model of the true components underlying the data, especially if we deal with very heterogeneous data. Part of the problem stems from the Markov property that the relationship among adjacent voxel pairs is determined by the input features (38). First order (four neighbors) and second order (eight neighbors) hierarchies of neighborhood systems are used (16). This makes the optimization problem very hard to solve because it requires a global adjustment and we deal with extremely high-dimensional data. We have shown that a computational cheaper approach for introducing spatial information can bring very satisfactory improvements in the quantification process. In our proposed adaptive method, AQSES-MRSI, a nonlinear least squares problem is solved only for the

parameters of the current signal for each voxel at a time, and several sweeps through the MRSI grid are performed so that some of the hyperparameters of the problem are optimized at each sweep. Hence, as opposed to previous studies (15, 16), a common optimization for simultaneously fitting all the signals in the MRSI grid and simultaneously penalizing all their parameters was not explicitly needed in this study.

Quantification methods based on numerical optimization usually require excellent starting values for the model parameters. With AQSES-MRSI an intrinsic correction mechanism, to adapt the starting values and to correct the non-linear parameters variability in the quantification of each signal at each sweep through the grid, is proposed. Thus, simply starting in the first sweep with zero corrections on the dampings and zero frequency shifts for all the metabolite profiles, still leaves the possibility of multi-start optimization, since starting values can change at each sweep according to the parameters of the neighboring voxels. The LCModel software package (10, 11) also offers the possibility to analyze MRSI data in one multivoxel run. It first analyzes a central voxel of the subset and then works outwards, using Bayesian learning to get starting estimates and "soft constraints" for the first-order phase correction and the referencing shift from the preceding central voxels for the outer voxels. Still no smoothing on the nonlinear parameters is imposed. As in (16) we show that by adding a smoothing penalty term an improved solution is obtained. Another added value of AQSES-MRSI is the fact that neighboring regions are dynamically chosen, giving the user the possibility to extend or to limit the neighborhood area by adding tissue prior knowledge when defining this area.

AQSES-MRSI, the methods proposed in (15, 16) and LCModel software have in common that the resolution of the parameter maps equals the resolution of the MRSI grid, although MRI information can be used for pre-assignment of voxels to a certain tissue type. An interesting different approach is considered by the recent *k*-space-time methods (17, 39),

which use prior anatomical knowledge to reconstruct MRSI signals and metabolic maps at the resolution of the underlying MRI.

5. Conclusions

A new automated method for the quantification of MRSI data, called AQSES-MRSI, which incorporates spatial information, is proposed. It uses simple spatial constraints on the nonlinear spectral parameters, while allowing total freedom to the metabolite weights. Results show that it significantly improves metabolite estimates of MRSI data and can provide easy-to-interpret metabolite maps, which in turn could further be exploited for tissue classification. We demonstrate how essential it is to have a robust method for tuning the starting values, the soft constraints and the additional penalties involved in the optimization algorithm.

Exploiting spatial prior knowledge is shown to improve the accuracy of quantification compared to processing MRSI voxels on an individual basis. It brings the advantage that overlapping peaks or peaks of compounds present at low concentration can be better resolved than in single-voxel approaches. Because of the automation of the method and its improved robustness to deal with spatial heterogeneity of spectral data, AQSES-MRSI is expected to be a better and more attractive tool to analyze clinical MRSI data, for patients with intracranial tumours, than single-voxel approaches. Future work involves evaluating the method in conjunction with MRI segmentation methods for voxel pre-assignment, an optimization of the smoothing functions for data with sharp tissue boundaries and its further application to *in vivo* 3D MRSI tumor studies.

Acknowledgments

Research supported by Research Council KUL: GOA-AMBioRICS, GOA MaNet, CoE EF/05/006 Optimization in Engineering (OPTEC), IDO 05/010 EEG-fMRI, IDO 08/013

Autism, IOF-KP06/11 FunCopt, several PhD/postdoc & fellow grants; Flemish Government: FWO: PhD/postdoc grants, projects, FWO-G.0321.06 (Tensors/Spectral Analysis), G.0302.07 (SVM), G.0341.07 (Data fusion), research communities (ICCoS, ANMMM); IWT: TBM070713-Accelero, TBM070706-IOTA3, PhD Grants; Belgian Federal Science Policy Office IUAP P6/04 (DYSCO, `Dynamical systems, control and optimization', 2007-2011); EU: ETUMOUR (FP6-2002-LIFESCIHEALTH 503094), Healthagents (IST–2004–27214), FAST (FP6-MC-RTN-035801), Neuromath (COST-BM0601). D.M. Sima is a postdoctoral fellow of the Fund for Scientific Research Flanders.

References

1. De Edelenyi FS, Rubin C, Esteve F, Grand S, Decorps M, Lefournier V, Le Bas JF, Remy C. A new approach for analyzing proton magnetic resonance spectroscopic images of brain tumors: nosologic images. Nature Medicine. 2000; 6 : 1287– 1289.
2. Stadlbauer A, Moser E, Gruber S, Buslei R, Nimsky C, Fahlbusch R, Ganslandt O. Improved delineation of brain tumors: an automated method for segmentation based on pathologic changes of ^{1}H-MRSI metabolites in gliomas. NeuroImage. 2004; 23 : 454-461.
3. Gruber S, Stadlbauer A, Mlynarik V, Gatterbauer B, Roessler K, Moser E. Proton magnetic resonance spectroscopic imaging in brain tumor diagnosis. Neurosurgery Clinics of North America. 2005; 16 : 101-114.
4. Luts J, Laudadio T, Idema AJ, Simonetti AW, Heerschap A, Vandermeulen D, Suykens JAK, Van Huffel S. Nosologic imaging of the brain: segmentation and classification using MRI and MRSI. NMR in Biomedicine. 2009; 22(4) : 374-390.
5. Wright AJ, Fellows G, Byrnes TJ, Opstad KS, McIntyre DJO, Griffiths JR, Bell BA, Clark CA, Barrick TR, Howe FA. 2009. Pattern recognition of MRSI data shows regions of glioma growth that agree with DTI markers of brain tumor infiltration. Magnetic Resonance in Medicine. 2009; 62 : 1646-1651.

6. Devos A, Lukas L, Suykens JAK, Vanhamme L, Tate AR, Howe FA, Majos C, Moreno-Torres A, Van der Graaf M, Arus C, Van Huffel S. Classification of brain tumours using short echo time 1H MRS spectra. Journal of Magnetic Resonance. 2004; 170 : 164-175.
7. De Vos M, Laudadio T, Simonetti AW, Heerschap A, Van Huffel S. Fast nosologic imaging of the brain. Journal of Magnetic Resonance. 2007; 184 : 292-301
8. Van der Veen WC, De Beer WC, Luyten PR, van Ormondt D. Accurate quantification of in vivo ^{31}P NMR signals using the variable projection method and prior knowledge. Magnetic Resonance in Medicine. 2005; 6 : 92-98.
9. Vanhamme L, Van den Boogaart A, Van Huffel S. Improved Method for Accurate and Efficient Quantification of MRS Data with Use of Prior Knowledge. Journal of Magnetic Resonance. 1997; 129 : 35-43.
10. Provencher SW. Estimation of metabolite concentrations from localized in vivo proton NMR spectra. Magnetic Resonanace in Medicine. 1993; 30 : 672-679.
11. Provencher SW. Automatic quantitation of localized in vivo 1H spectra with LCModel. NMR in Biomedicine. 2003; 14 : 260-264.
12. Slotboom J, Boesch C, Kreis R. Versatile frequency domain fitting using time domain models and prior knowledge. Magnetic Resonance in Medicine. 1998; 39(6) : 899-911.
13. Ratiney H, Sdika M, Coenradie Y, Cavassila S, van Ormondt D, Graveron-Demilly D. Time-domain semi-parametric estimation based on a metabolite basis set. NMR Biomed. 2005; 18(1) : 1-13.
14. Poullet JB, Sima DM, Simonetti AW, De Neuter B, Vanhamme L, Lemmerling P, Van Huffel S. An automated quantitation of short echo time MRS spectra in an open source software environment: AQSES. NMR in Biomedicine. 2007; 20 : 493-504.
15. Pels P. Analysis and Improvement of Quantification Algorithms for Magnetic Resonance Spectroscopy. PhD Thesis. Leuven, Belgium. 2005.

16. Kelm BM. Evaluation of Vector-Valued Clinical Image Data Using Probabilistic Graphical Models: Quantification and Pattern Recognition. PhD Thesis. Heidelberg, Germany. 2007

17. Bao Y, Maudsley AA. Improved Reconstruction for MR Spectroscopic Imaging. IEEE Transactions on Medical Imaging. 2007; 26 : 686-695.

18. Magalhaes A, Godfrey W, Shen Y, Hu J, Smith W. Proton magnetic resonance spectroscopy of brain tumors correlated with pathology. Academic Radiology. 2005; 12 : 51-57.

19. Howe FA, Barton SJ, Cudlip SA, Stubbs M, Saunders DE, Murphy M, Wilkins P, Opstad KS, Doyle VL, McLean MA, Bell BA, Griffiths JR. Metabolic Profiles of Human Brain Tumors Using Quantitative In Vivo 1H Magnetic Resonance Spectroscopy. Magnetic Resonance in Medicine. 2003; 49 : 223–232.

20. Frahm J, Bruhn H, Gyngell ML, Merboldt KD, Hänicke W and Sauter R. Localized proton NMR spectroscopy in different regions of the human brain in vivo. Relaxation times and concentrations of cerebral metabolites. Magnetic Resonance in Medicine.1989; 11 : 47–63.

21. Oros-Peusquens AM, Laurila M, Shah NJ. Magnetic field dependence of the distribution of NMR relaxation times in the living human brain. MAGMA. 2008; 21 : 131–147.

22. Kamada K, Houkin K, Hida K, Matsuzawa H, Iwasaki Y, Abe H, and Nakada. Localized proton spectroscopy of focal brain pathology in humans: significant effects of edema on spin-spin relaxation time. Magnetic Resonance in Medicine. 1994; 31 : 537–540.

23. Sima D, Van Huffel S. Separable nonlinear least squares fitting with linear bound constraints and its application in magnetic resonance spectroscopy data quantification. Journal of Computational and Applied Mathematics. 2007; 203 : 264-278.

24. Poullet JB. Quantification and Classification of Magnetic Resonance Spectroscopic Data for Brain Tumor Diagnosis. PhD Thesis. Leuven, Belgium. 2008.

25. Laudadio T, Pels P, De Lathauwer L, Van Hecke P, Van Huffel S. Tissue segmentation of MRSI data using Canonical Correlation Analysis. Proc. of the Second International Conference on Computational Intelligence in Medicine and Healthcare. Lisbon, Portugal. 2005.

26. Friman O. Adaptive Analysis of Functional MRI Data. PhD Thesis. Linköping Sweden. 2003.

27. http://azizu.uab.es/INTERPRET/

28. Naressi A, Couturier C, Castang I, De Beer R, and Graveron-Demilly D. Java-based graphical user interface for mrui, a software package for quantitation of in vivo/medical magnetic resonance spectroscopy signals. Computers in Biology and Medicine. 2001; 31 : 269–286.

29. Devos A. Quantification and classification of Magnetic Resonance Spectroscopy data and applications to brain tumour recognition. PhD Thesis. Leuven, Belgium. 2005.

30. Laudadio T, Mastronardi N, Vanhamme L, Van Hecke P, Van Huffel S. Improved Lanczos algorithms for blackbox MRS data quantitation. Journal of Magnetic Resonance. 2002; 157 : 292-297.

31. http://www.esat.kuleuven.be/~acroitor/InvivoAQSES-MRSI.doc

32. Maruyama I, Sadato N, Waki A. Hyperacute changes in glucose metabolism of brain tumors after stereotactic radiosurgery: a PET study. Journal of Nuclear Medicine. 1999; 40 : 1085–1090.

33. Fountas KN, Kapsalaki EZ, Gotsis SD, Kapsalakis JZ. In vivo proton magnetic resonance spectroscopy of brain tumors. Stereotactic and Functional Neurosurgery. 2000; 74 : 83-94.

34. Kinoshita Y, Yokota A. Absolute concentrations of metabolites in human brain tumors using in vitro proton magnetic resonance spectroscopy. NMR in Biomedicine. 1997; 10 : 2-12.

35. Kuesel AC, Donnelly SM, Halliday W, Sutherland GR, Smith ICP. Mobile lipids and metabolic heterogeneity of brain tumours as detectable by ex vivo 1HMR spectroscopy. NMR in Biomedicine. 1994; 7 : 172–180.

36. Vanhamme L, Van Huffel S, Van Hecke P, van Ormondt D. Time domain quantification of series of biomedical magnetic resonance spectroscopy signals. Journal of Magnetic Resonance. 1999; 140 : 120-130.

37. Chou PB, Brown CM. The theory and practice of Bayesian image labelling. International Journal of Computer Vision. 1990; 4 : 185-210.

38. Dietterich TG. Structural, Syntactic, and Statistical Pattern Recognition. Lecture Notes in Computer Science, chap. Machine Learning for Sequential Data 2396. 2007; 15-30.

39. Kornak J, Young K, Soher BJ, Maudsley AA. Bayesian *k*-Space-Time Reconstruction of MR Spectroscopic Imaging for Enhanced Resolution. IEEE Transactions on Medical Imaging. 2010; 29 : 1333-1350.

Captions of the figures

Figure 1: Visualization of the neighborhood regions (blue color) that is taken into account in the spatial model for the parameter map of the voxel of interest (red color). In a) the neighborhood contains all the voxels selected with the "3x3" spatial model. In b) the neighborhood contains only the voxels selected with the "3x3" spatial model and belonging to the same tissue class.

Figure 2: Simulated MRSI spectra reflecting normal brain tissue profile and presenting different levels of noise (SNR = 30, 25, 20, 15, 10 and a noise free case).

Figure 3: Mean of the RMSE amplitude values computed for the 25 simulated MRSI grids of 3x3 voxels, for different levels of SNR (30, 25, 20, 15, 10 and a noise free case); the influence on the performance of each step within the AQSES-MRSI algorithm.

Figure 4: Mean of the $RMSE_k$ amplitudes values computed for the 25 simulated MRSI grids of 3x3 voxels, for different metabolites. Vertical lines show the mean and the standard deviation values. SNR level is 25.

Figure 5: Mean of the $RMSE_k$ amplitudes values of Ala, Lac and Lip1 computed for the 25 simulated MRSI grids of 3x3 voxels for different levels of SNR.

Figure 6: a. Simulated MRSI grids with different parameter maps: A-D. 25% of the MRSI grid contains tumor like spectra (lower right corner) and 75% of the grid presents normal tissue like spectra. Color maps with the RMSE values for each voxel are presented for AQSES and AQSES-MRSI (see 2nd and 3rd row). In **b.** and **c**. the performance of AQSES-MRSI versus AQSES in estimating the metabolite concentrations for map D is detailed for each metabolite.

Figure 7: Metabolic maps obtained after applying QUEST, AQSES, AQSES-MRSI and LCModel. The color scheme is relative to each metabolite. The patient is diagnosed to have a meningioma (lower left corner of the MRI image).

Figure 8: Metabolic maps obtained after applying QUEST, AQSES, AQSES-MRSI and LCModel. The color scheme is relative to each metabolite. The patient is diagnosed to have a glioblastoma (upper right corner of the MRI image).

Figure 9: In a. metabolic maps obtained with AQSES-MRSI and LCModel for a patient diagnosed with oligoastrocytoma tumor grade III (upper left corner of the MRSI grid). The color scheme is relative to each metabolite. In b. the quantification results obtained with AQSES-MRSI, for 2 selected spectra: the residual, the fit and the signal are visualized. Upper signal comes from the tumor region; lower signal comes from the normal tissue area, as marked on the NAA map.

A new automated time-domain quantification method for MRSI data, which exploits the spatial information present in the data, is proposed. Overlapping peaks or peaks of compounds present at low concentration are better quantified with the proposed multi-voxel method than with single-voxel approaches.

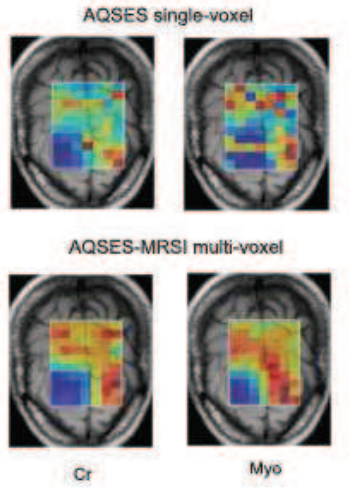

Exploiting spatial information to estimate metabolite levels in 2D MRSI of heterogeneous brain lesions

Anca R. Croitor Sava*, Diana M. Sima, Jean-Baptiste Poullet, Alan Wright, Arend Heerschap and Sabine Van Huffel

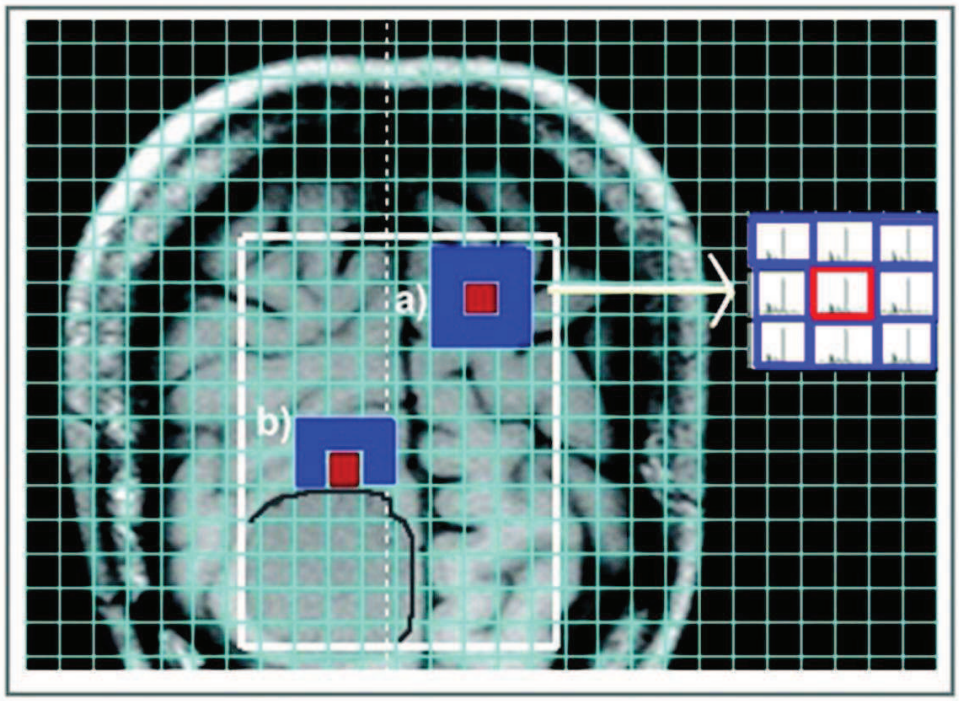

Figure 1: Visualization of the neighborhood regions (blue color) that is taken into account in the spatial model for the parameter map of the voxel of interest (red color). In a) the neighborhood contains all the voxels selected with the "3x3" spatial model. In b) the neighborhood contains only the voxels selected with the "3x3" spatial model and belonging to the same tissue class.
50x36mm (600 x 600 DPI)

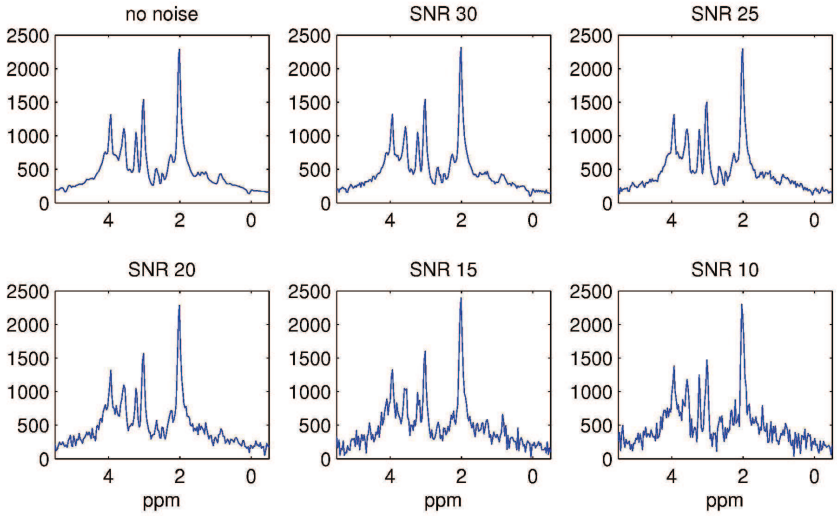

Figure 2: Simulated MRSI spectra reflecting normal brain tissue profile and presenting different levels of noise (SNR = 30, 25, 20, 15, 10 and a noise free case).
182x98mm (600 x 600 DPI)

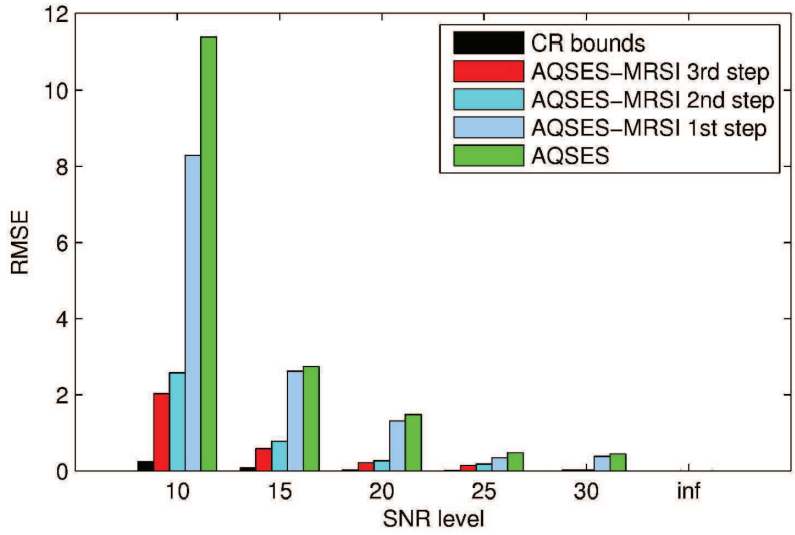

Figure 3: Mean of the RMSE amplitude values computed for the 25 simulated MRSI grids of 3x3 voxels, for different levels of SNR (30, 25, 20, 15, 10 and a noise free case); the influence on the performance of each step within the AQSES-MRSI algorithm.

154x93mm (600 x 600 DPI)

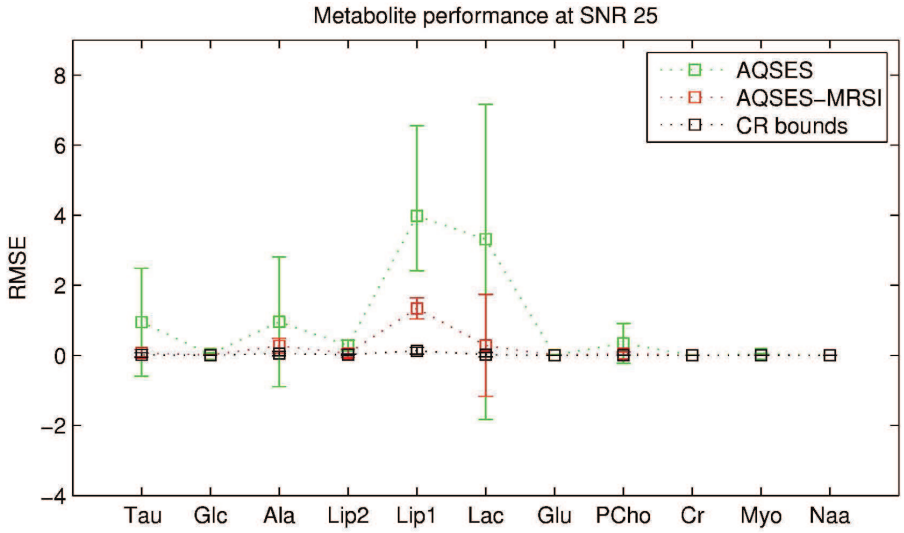

Figure 4: Mean of the RMSEk amplitudes values computed for the 25 simulated MRSI grids of 3x3 voxels, for different metabolites. Vertical lines show the mean and the standard deviation values. SNR level is 25.
157x83mm (600 x 600 DPI)

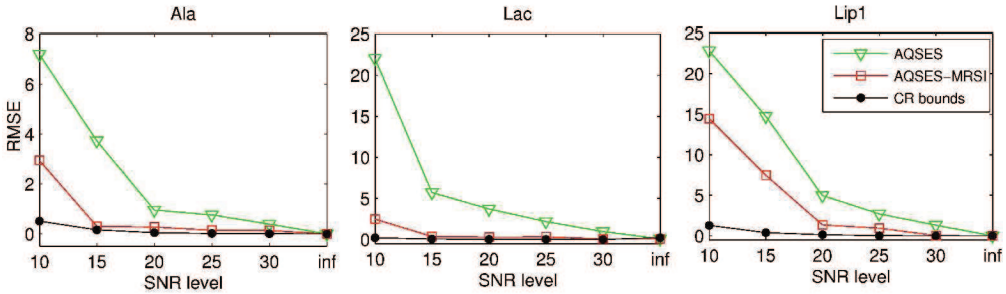

Figure 5: Mean of the RMSEk amplitudes values of Ala, Lac and Lip1 computed for the 25 simulated MRSI grids of 3x3 voxels for different levels of SNR.
198x65mm (600 x 600 DPI)

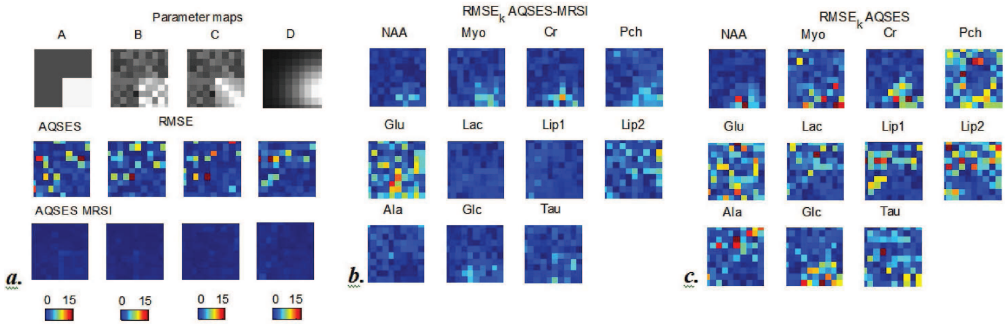

Figure 6: a. Simulated MRSI grids with different parameter maps: A-D. 25% of the MRSI grid contains tumor like spectra (lower right corner) and 75% of the grid presents normal tissue like spectra. Color maps with the RMSE values for each voxel are presented for AQSES and AQSES-MRSI (see 2nd and 3rd row). In b. and c. the performance of AQSES-MRSI versus AQSES in estimating the metabolite concentrations for map D is detailed for each metabolite.
124x41mm (600 x 600 DPI)

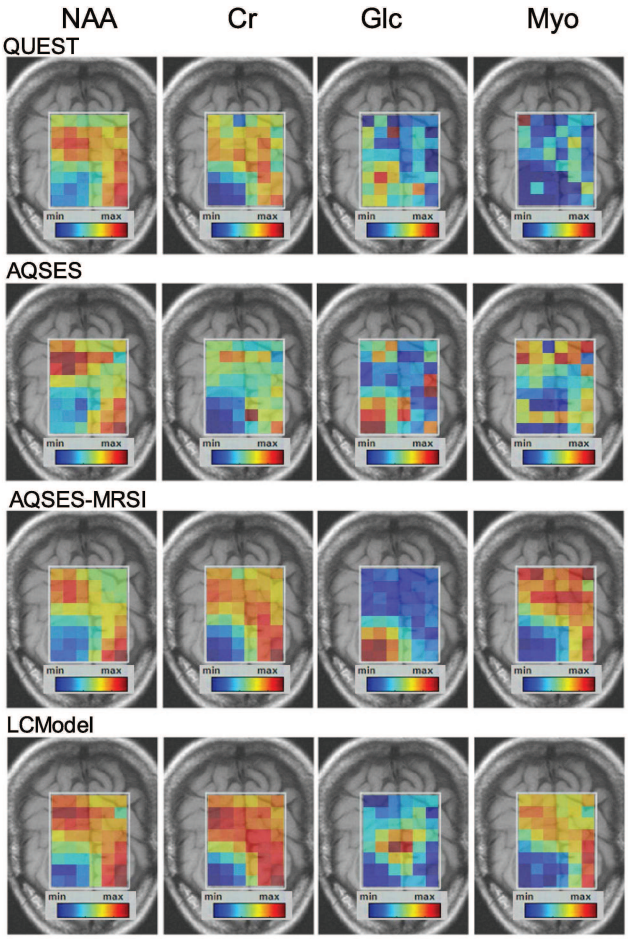

Figure 7: Metabolic maps obtained after applying QUEST, AQSES, AQSES-MRSI and LCModel. The color scheme is relative to each metabolite. The patient is diagnosed to have a meningioma (lower left corner of the MRI image).
126x158mm (600 x 600 DPI)

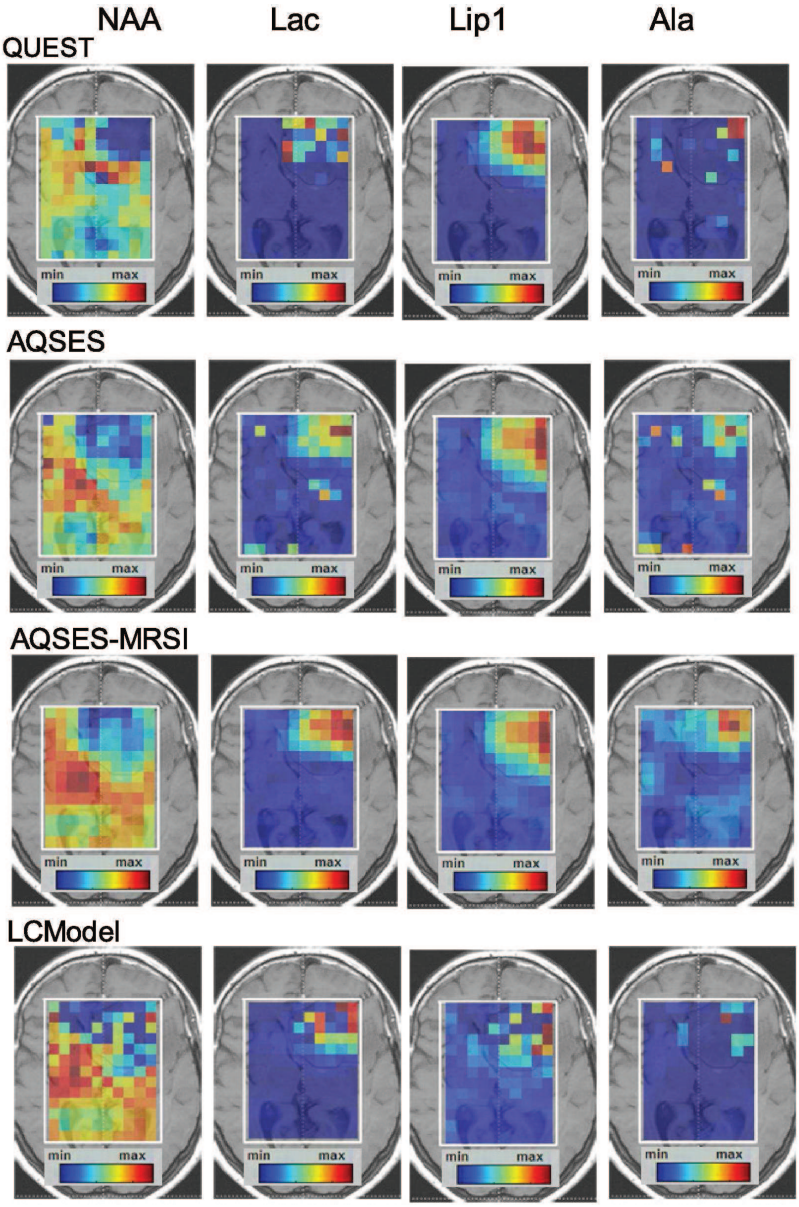

Figure 8: Metabolic maps obtained after applying QUEST, AQSES, AQSES-MRSI and LCModel. The color scheme is relative to each metabolite. The patient is diagnosed to have a glioblastoma (upper right corner of the MRI image).
82x102mm (600 x 600 DPI)

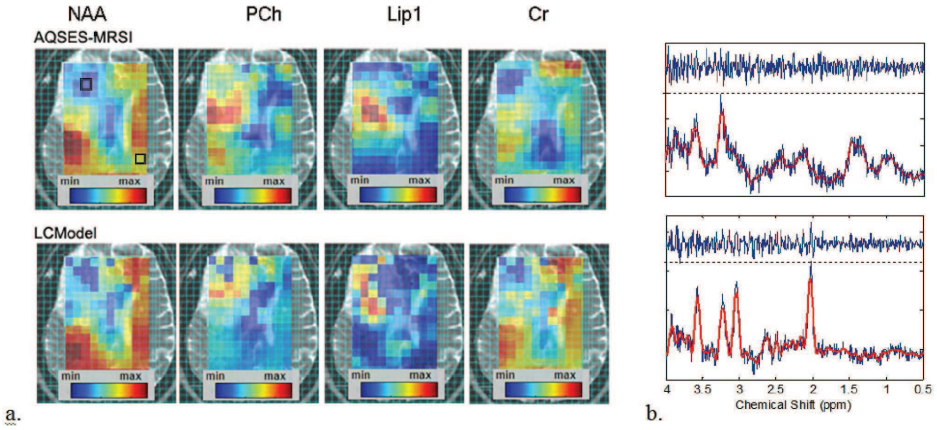

Figure 9: In a. metabolic maps obtained with AQSES-MRSI and LCModel for a patient diagnosed with oligoastrocytoma tumor grade III (upper left corner of the MRSI grid). The color scheme is relative to each metabolite. In b. the quantification results obtained with AQSES-MRSI, for 2 selected spectra: the residual, the fit and the signal are visualized. Upper signal comes from the tumor region, lower signal comes from the normal tissue area, as marked on the NAA map.
183x85mm (600 x 600 DPI)